Reviews

The effect of the shape of a mesogenic group on the structure of supramolecular aggregates based on wedge-shaped and cone-shaped dendrons

A. A. Stupnikov,[a,b] M. A. Shcherbina,[a,c] and S. N. Chvalun[a,c]

[a]National Research Center "Kurchatov institute",
1 pl. Akad. Kurchatova, 123182 Moscow, Russian Federation.
E-mail: max-shcherbina@yandex.ru
[b]Moscow Technological University, Institute of Fine Chemical Technologies,
86 prosp. Vernadskogo, 119571 Moscow, Russian Federation
[c]Enikolopov Institute of Synthetic Polymeric Materials, Russian Academy of Science,
70 ul. Profsoyuznaya, 117393 Moscow, Russian Federation

This review addresses the key principles underlying the formation of liquid crystalline phases based on wedge-shaped and cone-shaped dendrons of different chemical nature. Despite rich phase diversity of the above systems, the development of a mesophase can be reliably predicted by the geometric model, which compares the shape of a wedge dendron with the radial density distribution in the relevant Voronoi polyhedra. 2D columnar phases formed by chiral [7]-heterohelicene molecules with long aliphatic side chains are described in detail. The as-formed columnar aggregates are shown to possess a helical 13_2 symmetry and are composed of thirteen blocks, and each block involves six molecules. In this case, the internal structure of the first-level (lower) supramolecular aggregate appears to be different from that of the helical supramolecular structure.

Key words: self-assembly, wedge-shaped dendrons, liquid crystalline mesophases, rotational crystalline phases, plastic crystals, [7]-heterohelicene, Frank—Kasper phases, Kelvin problem.

Wedge-shaped dendrons serve as building blocks for most synthetic self-assembling systems.[1] Recently, a new class of wedge-shaped molecules (*cunitic* or *tapered mesogens*) has offered new promising benefits for the materials science because the above materials are characterized by a rich phase diversity: formation of thermotropic smectic, columnar, bicontinuous mesophases as well as mesophases like a plastic crystal.[2] The above dendrons can be functionalized by diverse chemical compounds, for example, ion-conducting crown ethers,[3] donor-acceptor complexes,[4] magnetic atoms, nanoparticles,[5] and peptides.[6] The temperature-induced phase transition of columnar to spherical aggregates can be used as a thermal switcher: at a given temperature, an ion or an electron-conducting wire

Published in Russian in *Izvestiya Akademii Nauk. Seriya Khimicheskaya,* No. 9, pp. 1547—1557, September, 2018.
1066-5285/18/6709-1547

would break down into isolated spherical fragments, thus opening the circuit.[1]

The universal feature of the above systems is concerned with the development of unorthodox mesophases. This behavior can be exemplified by the fact that wedge-shaped derivatives of gallic acid produce columnar aggregates with the helical structure 8_1 (in the polymer H12-ABG-PMA[7]) and 13_2 (in the macromonomer H12-ABG-OH) as well as a columnar mesophase with symmetry 12_0,[8] which is formed by alkaline salts of symmetric and non-symmetric benzenesulfonic acid. In the general case, rotation axes of this order are incompatible with a crystalline lattice of any type. Therefore, their existence can be provided only at a certain trade-off, for example, when the order correlation between neighboring columns is compromised. Hence, this is not a classical crystalline order but a partially ordered state, in which columnar supramolecular aggregates as unidimensional crystals are organized into a certain 2D crystalline lattice. However, this system lacks a long-range order because, in each supramolecular aggregate, the order is not correlated with the order in neighboring columns. These systems can be compared to a rotation crystalline phase, which is produced by several polymers.

Pioneering examples of "disordered hexagonal shape" in polymers have been discovered in the early 1960s for poly(tetrafluoroethylene) (PTFE) at a temperature above 30 °C[9,10] and 1,4-*trans*-polybutadiene ($T > 83$ °C).[11—13] By now, this mesophase has been revealed for several polymers.[14] The comprehensive review on this subject has been reported.[15] For polysiloxanes and polyphosphazenes, this shape has been discussed by Yu. K. Godovsky *et al.*[16] Basic features of a columnar mesophase in polymers are concerned with the lack of the long-range order along the chain axis and, correspondingly, 2D hexagonal packing of macromolecules.

Coming back to the development of aggregates of different helical symmetry, let us consider in more detail another fascinating case: formation of supramolecular aggregates of two levels by [7]-heterohelicene derivatives (compound **I**) with long aliphatic side groups. Many helicenes and heterohelicenes with long aliphatic side groups produce cylindrical supramolecular aggregates with a helical symmetry.[17—19] Specific features of these compounds are concerned with the fact that the initial molecules by themselves are helical. For many crystallizable helicenes, these molecules produce columns, which are located one on the top of the other. However, the presence of long aliphatic side groups in the chiral compound **I** prevents the formation of a truly crystalline order since, for the stable existence of a liquid crystalline (LC) columnar phase, the ratio of the volume of aliphatic side groups to the volume of an aromatic core of the column is too high. Hence, ordering of molecules **I** is organized into far more complicated and fascinating shapes. Racemic mixtures of enantiomers of compound **I** (hereinafter, **I-*rac***) and isolated pure enantiomer (hereinafter, **I-*l***) were described.[20]

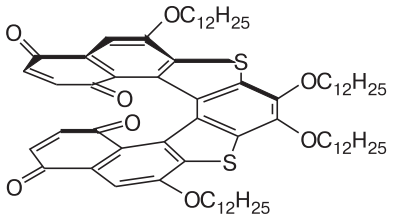

I

At room temperature, samples **I-*rac*** and **I-*l*** are highly ductile solid materials, which are characterized by the existence of an ordered 2D columnar mesophase with a melting temperature of 215 °C (40 kJ mol^{-1}) and 242 °C (47 kJ mol^{-1}), respectively. In this case, no other phase transitions were revealed by the POM, DSC, and SAXS methods. Specific features of the samples **I-*l*** are concerned with the phenomenon of circular fluorescence polarization[21] and the intensive second-harmonic generation.[22]

Figure 1, *a* shows the X-ray scattering pattern for the compound **I-*rac***. For the compound **I-*l***, the WAXS patterns appear to be nearly identical to those of **I-*rac*** and are not shown in the figure. For the above compounds, the difference between the SAXS patterns is concerned with the shape of the X-ray reflection 102 (this X-ray reflection is shown by the arrow in Fig. 1, *b*). The above data are typical of the X-ray scattering from the two-dimensional ordered columnar mesophase; in the SAXS scattering region, a set of narrow X-ray reflections is observed. In this case, the ratio of squared interplanar distances is equal to 1 : 3 : 4 : 7 : 9 : 12 : 13, which is characteristic of the 2D hexagonal mesophase ($a_{hex} = 4.0$ nm). At the same time, in the regions of the X-ray scattering corresponding to the wave vector modulus of 0.3—0.5 nm, only broad diffuse intensity maxima are observed, and these maxima are provided by the structure within a singular columnar supramolecular aggregate. They produce a triple cross, which is typical of X-ray diffraction of individual helical structures. Their centers lie along zeroth, thirteenth, and twenty-sixth layer lines. Noteworthy is that the zeroth and twenty-sixth layer lines show only the X-ray reflections with the even Miller index *l* (0, 2, 4, 24 (weak), 26), whereas the thirteenth layer line has the odd Miller index *l* (11, 13, 15, 17). This evidence suggests that the molecules of compounds **I-*rac*** and **I-*l*** produce continuous supramolecular columnar aggregates with the helical symmetry 13_2[23] and with the period along the axis of the column, which is equal to $c_0 = 11.1$ nm; one helix pitch is equal to 5.5 nm. If, as was expected earlier,[19,24,25] the molecules of the compound **I-*rac*** are arranged one on the top of the other in the column, then, one "elementary cell" should involve thirteen molecules. In this case, according to trivial calculations, density appears to be very low and equal to 0.16 g cm^{-3}; at the same time, the experimental value at

208 °C is six times higher and equal to (1.058±0.002) g cm^{-3}. This evidence suggests a complex structural organization of the heterohelicene columns. Moreover, the electron density distribution in the compound **I-*rac*** calculated from the relative intensity of the small-angle X-ray reflections (see Fig. 1, *c*) shows that the region with high electron density, which, in the system under study, can be presented only by aromatic fragments, occupies a higher volume as compared with the case where the molecules of the compound under study are arranged one above the other; nearly three diameters of an individual molecule in the plane perpendicular to the columnar axis. Let us also mention that, at the centers of columnar helical supramolecular aggregates, the regions with a very low electron density are located, and their radius is equal to several angstroms. As was shown earlier for other systems based on wedge-shaped dendrons,[2,8,26–31] the above dramatic downturn of the electron density corresponds to the presence of an open through channel in the columnar supramolecular aggregates.

According to the crystalline lattice parameters and macroscopic density of the material, one full period involves 78 helicene molecules. Hence, the relevant helix 13_2 composed of these molecules is expected to involve thirteen blocks, and each block contains six molecules. In this case, the inner structure of the (small-sized) supramo-

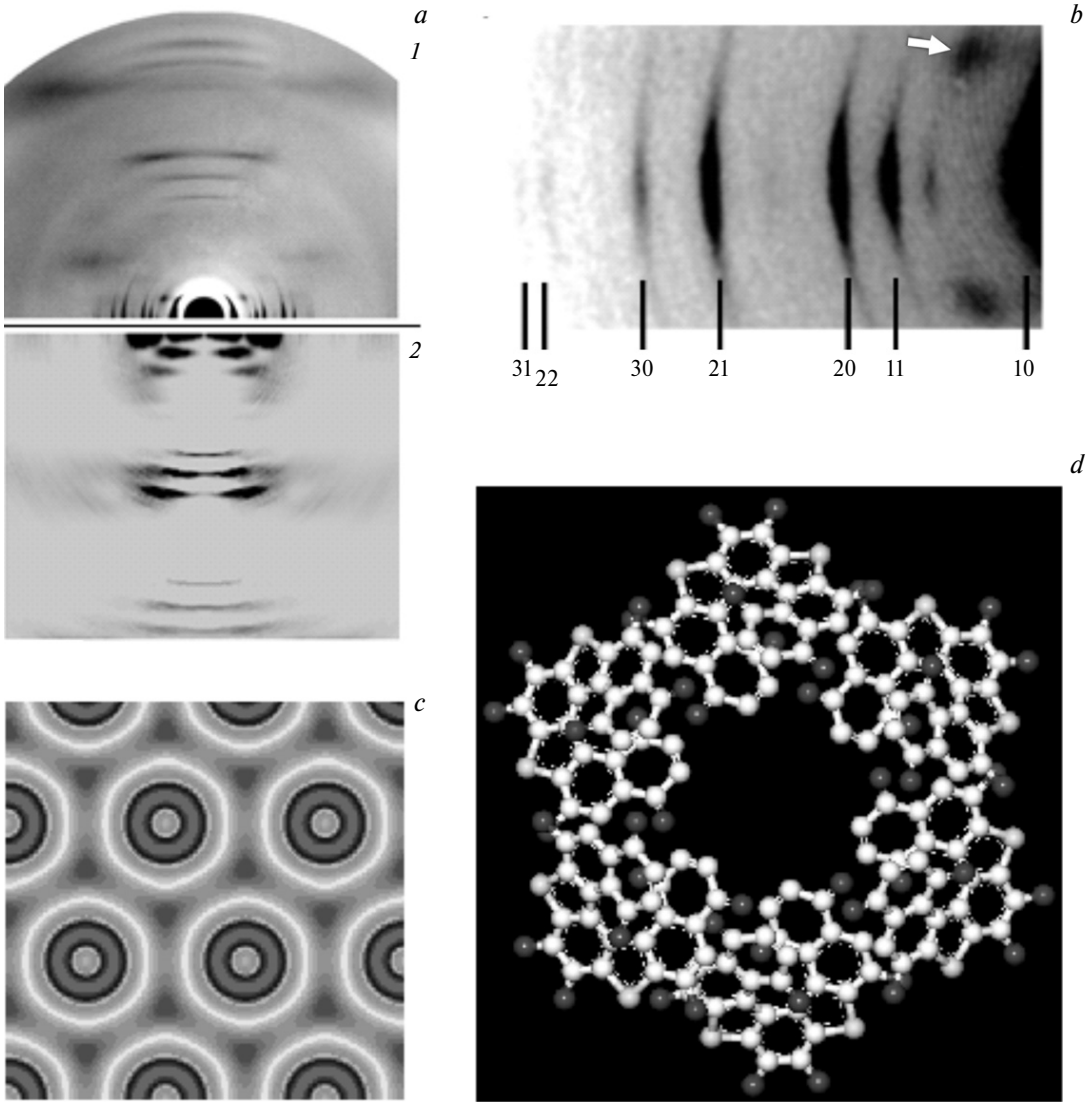

Fig. 1. (*a*) Experimental (*1*) and calculated X-ray scattering patterns for the helix 13_2 (*2*) for compound **I-*rac***, (*b*) enlarged small-angle X-ray scattering region (the indices for the X-ray reflections of the columnar phase), the arrow shows the reflection 102; (*c*) electron density distribution in the ordered columnar phase based on compound **I-*rac***, which is calculated from the relative intensity of the small-angle X-ray reflections; (*d*) a supramolecular aggregate composed of six molecules of 7-heterohelicene, basic unit of columnar supramolecular aggregates.

lecular first-level aggregate appears to be different from the structure of the helical supramolecular aggregate. The results of the simulation of X-ray scattering patterns (see Fig. 1, *a*; the mirror image at the bottom) show that the best fit with the experimental data is achieved for the aggregates, in which the center of gravity of each of six molecules is spaced from the axis by 7.8 Å, and the molecules by themselves are tilted with respect to the column axis by $\omega_0 = 30°$ (*tilt angle*); the angle of rotation of the molecules with respect to the helix radius (*fan angle*) is equal to $\rho_0 = 10°$, and the shift of the centers of gravity of the consecutive molecules along the column axis is equal to 1.7 Å. The above aggregates have the helical structure (see Fig. 1, *d*), which well fits the helix 13_2, into which they are arranged. Figure 1, *d* shows the general scheme of the supramolecular columnar aggregates based on the molecules of compounds **I-*rac*** and **I-*l***.

In the molecular simulation experiments performed for liquid crystalline systems in general and compound **I** in particular, one should take into account the disordered state of aliphatic tails. Any fixed conformation of the tails leads to the development of additional artifact X-ray reflections on the calculated X-ray scattering patterns. Therefore, the most expedient approach involves the simulation of the X-ray scattering patterns only for mesogenic groups (molecules, in which the aliphatic tails are substituted by hydrogen atoms). This approach allows the account for the basic characteristic features of the X-ray scattering patterns related to minor deviations of the relative intensity of the X-ray reflections due to changes in the mean electron density (aliphatic tails are neglected) and, correspondingly, distortions of the calculated contrast.

Noteworthy is that the packing of broader aromatic fragments of heterohelicene molecules at the centers of the columns provides comparatively high values of ρ_0 and ω_0. A comparatively strong diffuse scattering between the twenty-first and twenty-fourth layer lines of the experimental X-ray diffraction patterns (which is not reproduced in the calculated diffractograms) can be associated with disordered aliphatic tails with a minor tilt with respect to the radial plane of the column. The X-ray reflections on the non-zeroth layer lines feature the streaks, and this fact attests the absence of any marked order correlation between different columns. At the same time, the equatorial X-ray reflections are exceptionally narrow in the radial direction and well resolved due to the presence of the long-range order in the arrangement of columnar supramolecular aggregates in the 2D hexagonal lattice. Of special interest is a comparatively narrow X-ray reflection on the second layer line because only its appearance in the X-ray patterns of **I-*l*** and **I-*rac*** is different. In the first case, this X-ray reflection can be classified as (102); however, in the X-ray patterns of the racemate, this reflection is shifted away from the meridian along the layer line and is not compatible with the 2D hexagonal lattice.

Therefore, even the racemic mixture of compound **I** has a certain long-range order in the correlation of helical symmetry along neighboring columnar supramolecular aggregates. However, their interaction is not well pronounced because no other non-equatorial X-ray reflections related to the correlation of neighboring sites of the 2D hexagonal lattice are detected. This ordering is likely to be developed between the enveloping supramolecular aggregates rather than between certain molecules involved in the aggregates. Noteworthy is that, in an ideal 3D lattice composed of helical columns with similar twisting direction, there exists a certain ordering in the longitudinal and angular position of these columns with respect to each other. However, in the racemic mixture, right-handed molecules produce right-handed helical columns, whereas the left-handed molecules - left-handed columns. In the general case, when the ratio of the number of helical aggregates with different rotation direction is equal 1 : 1, the symmetry of the crystalline lattice decreases down to triclinic. However, in certain cases, a monoclinic or orthorhombic lattice can be formed as in the alpha-form of isotactic polypropylene.[32,33]

Another important class of wedge-shaped and cone-shaped dendrons is concerned with the compounds based on gallic acid.[34] From the early 1990s, comprehensive studies[35–41] on the compounds based on bulky wedge-shaped 3,4,5-tri(*n*-iloxybenzyloxy)benzoate have been conducted. The above-mentioned compounds have different length of alkyl radical $R = -(CH_2)_{n-1}-CH_3$ ($n = 10$, 12, 18 carbon atoms), and this alkyl radical can be partially fluorinated, $R = -(CH_2)_{n-m}-(CF_2)_{m-1}-CF_3$.

Certain representatives of this class of compounds show the tendency for self-assembly into supramolecular cylinders. In turn, these cylinders in the bulk state are organized either into the 2D ordered phase Col_{ho} or into the disordered columnar LC phase Col_h[35–37]. In this case, the first phase is characterized by ordering only inside each individual column in the absence of any correlation between neighboring columns. The internal structure of the columns with characteristic tilted mesogenic groups (the pine tree structure) is primarily controlled by the interaction between these groups.

For rigid wedge-shaped dendrons with different modifications, the effect of the shape of a sub-unit on the type of self-assembling structure has been revealed. The wedge-shaped form of the dendron is found to be transformed into the cone-shaped form due to the increase in the number of generation as well as due to the addition of alkyl tails at positions 4 and 3, 5 of the benzene ring. It is known that when the cross section of the mesogenic group S in the dendron increases in the proportion to the distance from the focal point r, the dendron is a flat object, for which the formation of a columnar phase is typical.[42] When the cross section area of the mesogenic group increases in proportion to r^2, the dendron acquires a cone-shaped form.

The cone-shaped dendrons are typically organized into micelles, which, in turn, produce mesophases like plastic crystals of various symmetries,[24,25] cubic phases $Im\bar{3}m$[16,17] and $Pm\bar{3}n$[17,43,44] as well as tetragonal phase $P4_2/mnm$[43]. Plastic crystals are mesophases with the maximum order. Their molecules or groups are disordered with respect to one or several axes but preserve their position; usually, this lattice is either cubic face-centered or body-centered.

As the temperature increases, the peripheral region of the wedge-shaped monodendrons can become broader, thus leading to the formation of micellar mesophases; when the extended rodlike shape is preserved, bicontinuous mesophases are formed.[8,34,45] As was mentioned above, spherical micelles involved in the formation of a plastic crystal can be organized not only by a single molecule but also by their supramolecular ensemble. For example, for the compounds with cunitic molecules, diverse micellar liquid crystalline phases are typical: cubic phase $Pm\bar{3}n$ (eight spherical micelles per one cell; in metallurgy, this phase is known as A15); tetragonal phase $P4_2/mnm$ (so-called σ-phase; thirty micelles per one cell); body-centered cubic phase $Im\bar{3}m$ (two micelles per one cell); aperiodic dodecagonal liquid quasi-crystals.[1,19,42,46] The phase $Pm\bar{3}n$ is the most common cubic mesophase and (84% of all micellar phases); note that 55% of all LC phases are observed in such compounds, including columnar and smectic mesophases.[1] At the same time, the body-centered crystalline lattice with the symmetry $Im\bar{3}m$ is characteristic of only 2% of possible cases. Below, we will try to explain the incidence of the formation of different LC phases in the systems.

Phases $Pm\bar{3}n$, $P4_2/mnm$ and $Fd\bar{3}m$ belong to so-called Frank-Kasper phases and are characterized by the close tetragonal packing.[47] There are known 24 Frank-Kasper phases in the melts of transition metals. Let us consider, as a general example, a well-known problem concerning the packing of solid spheres in a common lattice with the minimal free volume. The solution of this problem is provided by two close packings: face-centered cubic packing (Fig. 2, *a*) and closely packed hexagonal packing (see Fig. 2, *b*). In these packings, the existing spacings have tetragonal (see Fig. 2, *c*) and octahedral form (see Fig. 2, *d*). In this packing, the center of the octahedron is located at

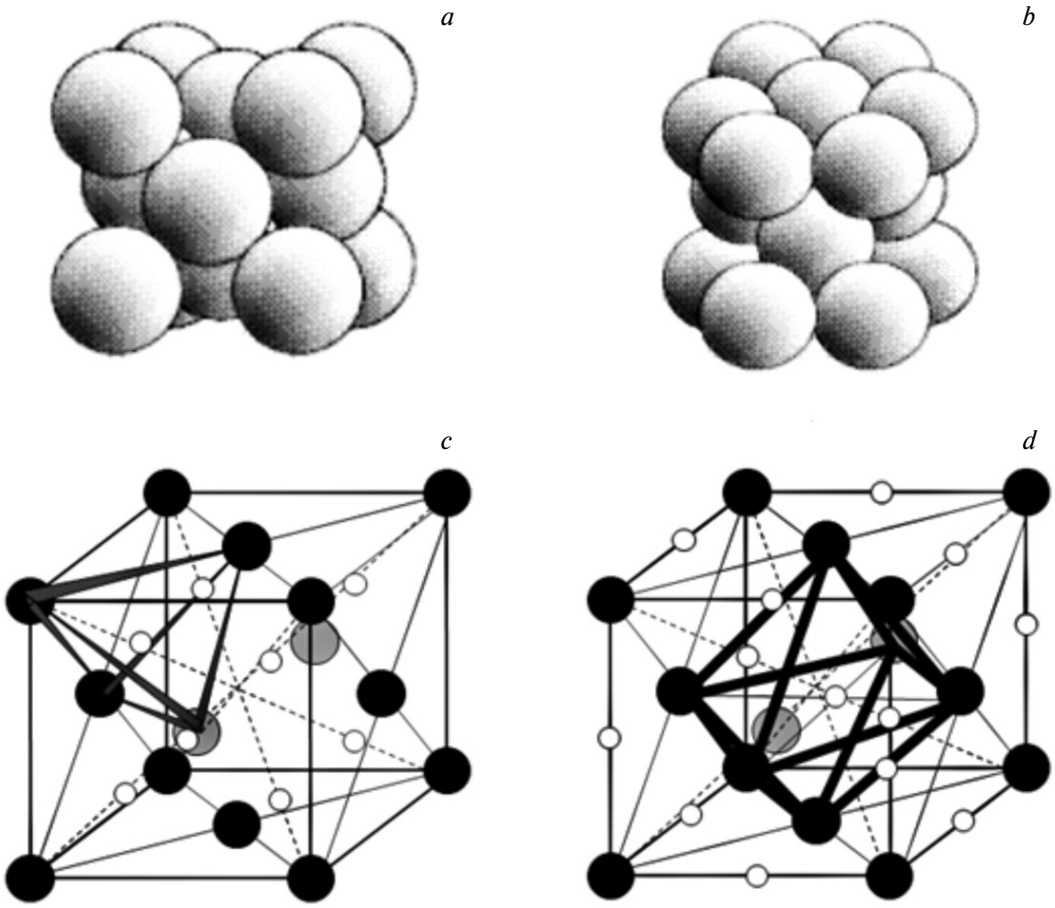

Fig. 2. Schemes of cubic face-centered (*a*) and hexagonal dense packing of spheres (*b*), tetragonal (*c*) and octahedral (*d*) spacings in such packings.

a higher distance from neighboring spheres than the center of the tetrahedron.

Each atom of face-centered cubic and hexagonal dense lattices has the coordination number of 12, and the coordination polyhedron has 6 square and 8 triangular faces and 34 vertices. If we consider a purely tetrahedral packing, one vertex appears to be adjoined by 5.1 tetrahedra. Hence, to accommodate the even number of tetrahedra, they should be stretched. If we consider the packing of icosahedra, the coordination number of their central atom is also equal to 12. However, the polyhedron involves only triangular faces and 30 vertices. This fact implies that, within this organization, the packing density of atoms is higher than that in the face-centered cubic or hexagonal closely packed phases. They have 30 rather than 24 close contacts. Due to the distortion of tetrahedra, the distance from the central atom to outer (shell) atoms is by 10% lower than that between the shell atoms. As was shown,[47] icosahedral packing well fits soft spheres because compression by 10% can be neglected. However, this packing appears to be most applicable also for 13 spheres because icosahedra are unable to occupy the whole space. The icosahedron has the pointlike symmetry $5\bar{3}(2/m)$ and can be compared to pentagonal antiprism with the outwards stretched centers of pentagons; as a result, vertices 11 and 12 are formed. Therefore, when icosahedra are arranged together with each other, the same problem concerning the space occupation, as in the case of pentahedra on the plane, arises. Nevertheless, it appears that all phases are layered, except two Frank—Kasper phases, which occur in melts. These layered phases involve alternating closely packed and loosened layers of atoms. Despite the fact that all Frank—Kasper phases contain the distorted icosahedra; they can also contain some other polyhedra with coordination numbers of 14, 15, and 16.[47] In crystallography, a coordination polyhedron is usually substituted by its topological pair, namely, by the tesselated Voronoi and Wigner—Seitz polyhedra.[48] For example, the Voronoi cell for the coordination icosahedron is a pentagonal dodecahedron. The Voronoi polyhedra corresponding to the coordination numbers 14, 15, and 16 contain 2, 3, and 4 hexagonal faces, respectively, in addition to 12 pentahedra. The cell of the phase $Pm\bar{3}n$ contains Voronoi 12-hedra and six 14-hedra.[49] For the dendron based on benzyl ether with alkoxy tails, the cell of the phase $P4_2/mnm$ is presented by isoelectron surfaces, which involve high-density aromatic dendrite cores, and enveloping Voronoi polyhedra. From 30 polyhedra producing the crystalline lattice, 10 of them are 12-hedra, sixteen— 14-hedra and four — 15-hedra. All the above polyhedra are somehow distorted, and two types of different distortions exist in 12-hedra and 14-hedra. As a result, 30 polyhedra feature five different coordination media. As will be shown below, analysis of the geometric shape of a dendron allows the prediction of the phase state of the material because the involute of the dendron shape coincides with the function of the radial distribution of coordination media (the Voronoi polyhedra) for a certain elementary cell of a plastic crystal. The presence of five different coordination media implies that the dendrons based on benzyl ether with alkoxy tails are able to produce simultaneously five different forms of micelles. In turn, this fact suggests a well-pronounced ability of the above dendrons for shape adaptation due to conformational changes of alkoxy groups. A far more pronounced difference in the micellar dimensions was found for the phase $Fd\bar{3}m$,[50] in which the Frank—Kasper structure is formed by the inverted micelles with the coordination numbers of 12 and 16, respectively. In the Frank—Kasper phases, the layers of atoms are composed of triangles, squares, and hexahedra. Triangles produce the faces of polyhedra with different coordination numbers. In phases $Pm\bar{3}n$ and $P4_2/mnm$, pentagonal surfaces are tilted with respect to basic layers and do not form continuous surfaces; in this way, the packing of pentahedra in periodic 3D structures is mastered.[47]When spheres are packed into a cubic lattice, the problem of their effective accommodation arises; however, packing of soft and semisoft spheres is challenged. This challenge has been accepted by Lord Kelvin in the XIXth century: he considered the efficient packing of soap bubbles in a soap foam with minimal surface. His interest to the soap foam was triggered by his assumptions that an extended gas-free foam has zero modulus and, hence, it can serve as a fair mechanical model for ether of space, which was supposed to carry the light waves without a longitudinal component.[47]

The reasons why metals and dendrimers adopt equivalent complex types of packing are related to the fact that spheres within the crystalline lattice are sufficiently soft. Softness of atomic *d*-orbitals plays an important role for the tetragonal close packing in the transition metals. Supramolecular aggregates can be visualized as rigid spherical cores with soft aliphatic crowns. In these systems, the solution of the problem of optimal packing coincides with the solution of the Kelvin problem on the minimization of the surface energy of a dry foam (minimal surface per a bubble). Lord Kelvin proposed the body-centered cubic mesopahe with symmetry $Im\bar{3}m$; however, the cubic structure with symmetry $Pm\bar{3}n$ occupies a smaller space by 0.4%.[51] In many supramolecular dendrimers and other liquid crystals, the frequency of the formation of the packing with symmetry $Pm\bar{3}n$ as an equilibrium structures was credited as an experimental proof of the the Weaire—Phelan structure. At the same time, as at high temperatures, enhanced conformational disorder leads to the lateral expansion of the dendrimer aliphatic crown; at low temperatures, the driving force is concerned with the minimization of free surface.

Noteworthy is that the dendron shape plays the most crucial role for the shape of a self-assembling micelle and, hence, for the structure and symmetry of the formed

liquid crystalline phase. Let us consider the functions of radial volume distribution for different 3D-structures.[47] Consider a sphere with a variable radius r, when the center of the sphere coincides with the center of the corresponding Voronoi polyhedron. If $v_i(r)$ is assumed to be the part of the volume of the i-th crystalline cell inside the sphere, then, at low r, the sphere increases smoothly, and the ratio dV/dr is proportional to r^2. Once the sphere approaches the boundaries of the Voronoi polyhedra, further increase in the radius leads to the decrease in the volume growth rate.

If we consider the projection of a cone-shaped molecule (Fig. 3, *a*) on a plane perpendicular to the cone axis (see Fig. 3, *b*), the line enveloping the complete involute of the dendron can be described by the function dV/dr. In Fig. 3, *b,* the rectangular shows the region, for which the radial distribution functions corresponding to the dendrons with an ideal shape producing crystalline lattices of different symmetry are calculated. This model proves its efficiency for the prediction of self-assembly of the cone-shaped dendrons with different structures. For example, for the phase $Im\bar{3}m$, the volume distribution function has a sharper peak and a more dramatic decline at high r as compared with phases $Pm\bar{3}n$ and $P4_2/mnm$. This reasoning explains the formation of the phase $Im\bar{3}m$ from the above two phases upon heating due to the compression of alkyl tails of the dendron, which is provided by the increase in the content of *gauche* conformations.[25] Even though for the phases $Pm\bar{3}n$ and $P4_2/mnm$, volume distribution is nearly the same, and both phases often coexist, in the samples under study, as the temperature decreases, the

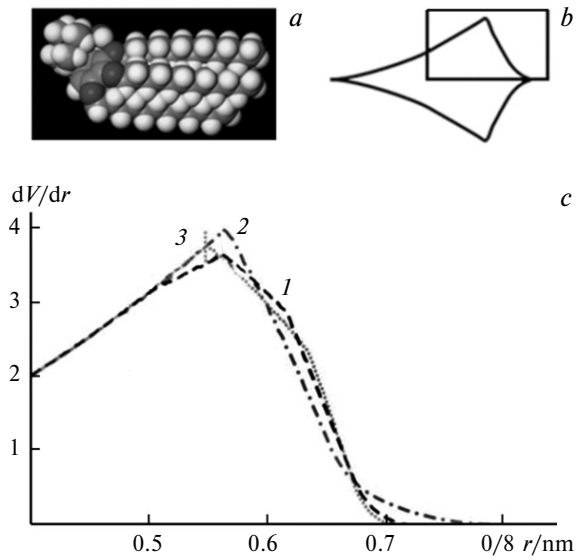

Fig. 3. (*a*) The example illustrating the cone-shaped monodendron based on benzene sulfonic acid; (*b*) projection of the envelope of the monodendron onto the plane perpendicular to the cone axis; (*c*) functions dV/dr pcalculated for different 3D micellar structures: $Pm\bar{3}n$ (*1*); $Fm\bar{3}m$ (*2*), $Im\bar{3}m$ (*3*).

structure like $Pm\bar{3}n$ is formed. However, the calculation of a more sensitive derivative $d\Omega/dr = d/dr[(1/r^2)(dV/dr)]$ allows the identification of this difference. This function describes the decrease in the mean solid angle (the angle formed by the untruncated part of the sphere in the Voronoi polyhedron). The shape of the curve $d\Omega/dr$ at r close to r_0 is especially important due to high repulsion between alkyl tails of spheres. This repulsion becomes weaker if the alkyl tails can be shifted with a slight gain in enthalpy. Therefore, phases with a higher content of close contacts are formed at lower temperatures or at a lower content of entanglements of alkyl tails of dendrons. Using the plot of the distribution dV/dr, one can explain why, for the cone-shaped dendrons, no cubic densely packed phase with symmetry $Fm\bar{3}m$ is formed. For an ideal form of the dendron, at high r, the observed high peak and a continuous function decay are allowed. To provide the formation of the phase with symmetry $Fm\bar{3}m$, the molecule should contain the branch at one of the first carbon atoms in alkyl tails and sufficiently long alkyl tails, which are able to fill the octahedral vacancies between the Voronoi polyhedra.[42]

To prove the efficiency of the geometric approach for the self-assembly of wedge-shaped monodendrons, monodendrons based on salts of tris(alkyloxy)benzenesulfonic acid with different modifications of alkyl end (**II**—**IV**) were synthesized and studied: with high dendron involute angle (Ω); with the modification of alkyl chains by additional branching into three new chains; with unequal length of alkyl chains.

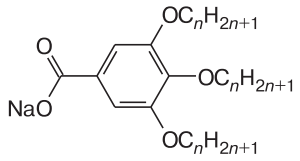

II

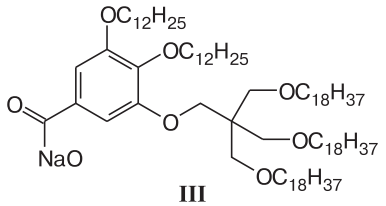

III

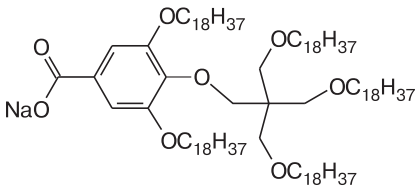

IV

According to the analysis of the volume radial distribution function dV/dr, branching of the peripheral region should lead to the formation of the body-centered cubic

mesophase. This hypothesis was proved for hyperbranched monodendrons of type AB5.[1] Upon heating, these monodendrons produce a body-centered cubic micellar mesophase. In such monodendrons, the introduction of non-branched alkyl tails, in addition to branched ones, assists the formation of intermediate mesophases (for example, columnar hexagonal mesophase for compound **IV**) prior to the transition to the body-centered cubic mesophase. For monodendrons with unequal length of alkyl chains (**III**), the size of the formed sphere is controlled by short alkyl tails and is equal to the size of the sphere of the monodendron **II**; in this case, longer alkyl tails **III** are folded or entangled, thus expanding the dendron. As the temperature increases, monodendrons are reorganized; they are expelled from micelles due to the widening of the peripheral part and, correspondingly, micelles of smaller diameter are formed.

To estimate the formed phases depending on divergence of a wedge-shaped molecule, the following approach appears to be efficient. Let us consider the dependence of the radial distribution of the dendron as a power function of the micellar radius: $dV/dr = kr^p$. Depending on the coefficient p, one can predict, with a certain error, the developed phases: $p \approx 0$, smectic phase; $0 < p < 1$, bicontinuous cubic phase; $p \approx 1$, columnar phase; $p \approx 2$, micellar phase (cubic or other symmetries). In whole, it should be mentioned that, at high values of the coefficient p, the development of a body-centered cubic mesophase is the most probable; at lower temperatures, plastic crystals with symmetry $Pm\bar{3}n$ are formed.[1]

Temperature variations also exert a predictable effect on the shape of a monodendron. At higher temperatures, the content of *gauche*-conformations in side chains increases, they are extended in the lateral direction and shrink down along the longitudinal direction. The monodendron becomes cunitic, thus favoring the phase transition from the columnar to cubic mesophase. If dendrons are covalently attached to the polymer chain and their expulsion from the columnar aggregates is impossible, the macrofiber extends upon heating in contrast to the conventional shrinkage of polymeric fibers.

Let us consider in brief possible applications of diverse self-assembling 2D and 3D ordered structures. The development of hyperbranched dendrons allows encapsulation of big-sized molecules and nanoparticles within spherical micelles and these micelles can be used as nanoreactors for the formation of nanoparticles.[1]

Organic molecules with their terminal groups are able to be attached to diverse substrates such as metals,[52—55] their oxides,[56 57] semiconductors, [58] *etc.*, and can be spontaneously assembled on their surface into the 2D lattices. The outer tails of the molecules in the monolayer can be somehow functionalized; as a result, properties of the surface are changed: the surface becomes either hydrophilic or hydrophobic,[59] and the surface state of a semiconductor is changed.[60] In microelectromechanical systems (MEMS), the self-assembling monolayer can reduce the friction of moving elements and protective coatings[61] and improve the reliability of microactuators and sensing structures.

The phenomenon of self-assembly allows one to control the position of a monolayer on a substrate as well as the positions of various elements with respect to the monolayer. Hence, these structures seem to be promising for electron industry. Nowadays, the self-assembling monolayers are used as ultrahigh-density storage carriers,[62], molecular wires, ionic channels.[63] Moreover, they are characterized by a negative differential resistance.[64] Many organic molecules have characteristic absorption spectra, especially, in the IR region, thus offering their practical application in optoelectronic devices.

Another essential route for the application of self-assembling monolayers with a uniform thickness of several nanometers is concerned with their ability to cover large surface areas, including those with a non-uniform profile. Hence, they can be used for the microcontact printing,[65] scanning probe lithography, atomic[66] or electron[67] beam (e-beam) lithography, photolithography.[68] For example, the method of microcontact printing with the use of poly(dimethylsiloxane) template was applied for the patterning of organoelectron chains,[69], patterning of biological objects on substrates,[70] as well as uneven substrates.[71] A wider application of self-assembled monolayers in lithography requires the solution of three basic problems: reduced imperfection of 2D crystalline lattice, mitigation of surface diffusion, and a broader scope of post-processing treatments.

As was mentioned above, the basic principle of self-assembly is concerned with the mutual ordering of elements under the action of weak non-covalent interactions when their energy does not markedly exceed the energy of thermal motion. As a result, self-assembled objects are highly sensitive to external impact and allow researchers and engineers to perform an accurate control over the structure of the material. For example, self-assembly under the action of the external electric field allows orientation of nanoconducting channels on the substrate surface.[72] Electric field was also used for the control over structural orientation in the films of block copolymers.[73] By varying the geometry of microchannels, one can achieve changes in the mutual packing of spherical colloidal nanoparticles.[74] For self-assembling aggregates containing magnetic nanoparticles, which produce photon crystals, structural changes under the action of magnetic field were observed.[75]

Let us mention another interesting class of compounds produced by self-assembly, nanoporous materials. Once 2D or 3D ordered matrix based on organic molecules is prepared, the material is subjected to thermooxidative destruction, mineralization, carbonization, and, if neces-

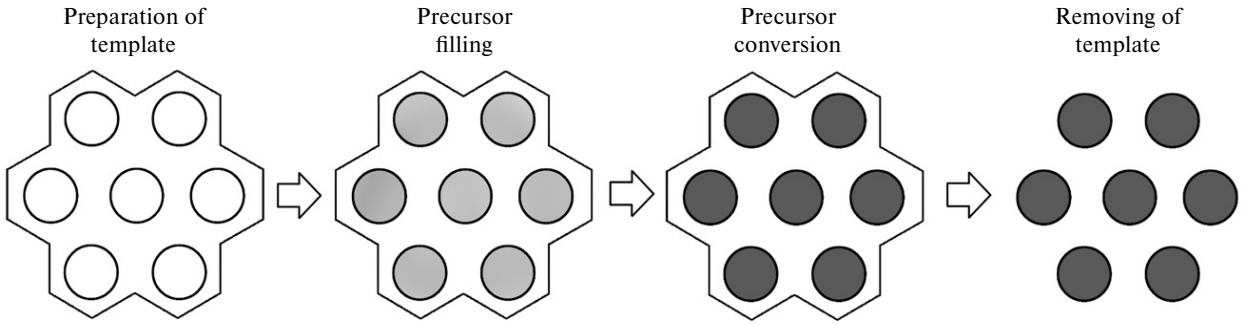

Fig. 4. General principle for the formation of nanoporous materials.

sary, crosslinking of the remaining framework (Fig. 4). As a result, the material with ordered pores is formed; pore dimensions, shape, and morphology can be tailored at the stage of the development of a self-assembling architecture.[76—84] The resultant carbon-based materials are characterized by an exceptionally high specific surface, low cost, chemical inertness, and fair mechanical properties. These materials can be used as sorbents, gas storage materials, semipermeable membranes. in electrodes and duodielectric chemical capacitors.[85,86] The complete list of different protocols for the development of mesoporous materials was presented elsewhere.[87]

For wedge-shaped liquid crystalline salts based on benzyl ammonium salts, it is possible to control ionic conductivity due to the reversible phase transition from orthogonal columnar to hexagonal columnar mesophase. In the columnar hexagonal phase, ionic conductivity is by four orders of magnitude higher than that in the orthorhombic columnar phase. According to the X-ray analysis data, conductivity in the orthorhombic columnar mesophase decreases due to the highly ordered arrangement of ions at the center of columnar aggregates.[88] Cations and anions occupy fixed positions inside the orthorhombic columnar structure and are immobile.

Despite phase diversity of rigid wedge-shaped and cone-shaped dendrons of different symmetry, the development of a certain mesophase can be predicted with a high accuracy by the geometric model, which provides the correlation between a shape of a rigid dendron and radial density distribution function in the corresponding Voronoi polyhedra. 2D columnar phases based on chiral molecules of [7]-heterohelicene with long side aliphatic substituents have the helical symmetry 13_2 and are composed of thirteen blocks, and each block involves six molecules. In this case, the inner structure (small-sized) supramolecular first-level aggregate is different from the structure of the supramolecular aggregate, a helix formed by the above aggregates.

This work was supported by the Russian Foundation for Basic Research (project no. 18-03-00967).

References

1. X. Yao, L. Cseh, X. Zeng, M. Xue, Y Liu, G. Ungar, *Nanoscale Horiz.*, 2017, **2**, 43.
2. M. A. Shcherbina, A. V. Bakirov, U. Beginn, L. Yan, X. Zhu, M. Möller, S. N. Chvalun, *Chem. Commun.*, 2017, **53**, 10070.
3. V. S. K. Balagurusamy, G. Ungar, V. Percec, G. Jhoanson, *J. Am. Chem. Soc.*, 1997, **119**, 1539.
4. T. T. Steckler, X. Zhang, J. Hwang, R. Honeyager, S. Ohira, X.-H. Zhang, A. Grant, S. Ellinger, S. A. Odom, D. Sweat, D. B. Tanner, A. G. Rinzler, S. Barlow, J.-L. Brédas, B. Kippelen, S. R. Marder, J. R. Reynolds, *J. Am. Chem. Soc.*, 2009, **131**, 2824.
5. B. M. Rosen, C. J. Wilson, D. A. Wilson, M. Peterca, M. R. Imam, V. Percec, *Chem. Rev.*, 2009, **109,** 6275.
6. K. T. Al-Jamal, C. Ramaswamy, A. T. Florence, *Adv. Drug Deliv. Rev.*, 2005, **57**, 2238.
7. V. Percec, C.-H. Ahn, W.-D. Cho, A. M. Jamieson, J. Kim, T. Leman, M. Schmidt, M. Gerle, M. Möller, S. A. Prokhorova, S. S. Sheiko, S. Z. D. Cheng, A. Zhang, G. Ungar, D. J. P. Yeardley, *J. Am. Chem. Soc.*, 1998, **120**, 8619.
8. M. A. Shcherbina, A. V. Bakirov, A. N. Yakunin, V. Percec, U. Beginn, M. Möller, S. N. Chvalun, *Crystallogr. Reports*, 2012, **57**, 151.
9. E. S. Clark, L. T. Muus, *Kristallogr., New Cryst. Struct.*, 1962, **117**, 119.
10. E. S. Clark, *J. Macromol. Sci., Part B*, 1967, **1**, 795.
11. G. Natta, P. Corradini, *Nuovo Cimento.*, 1960, **15**, 9.
12. K. Suehiro, M. Takayanagi, *J. Macromol. Sci.*, *Part B*, 1970, **4**, 39.
13. J. Finter, G. Wegner, *Macromol. Chem.*, 1981, **182**, 1859.
14. G. Ungar, *Polymer*, 1993, **34**, 2050.
15. B. Wunderlich, M. Möller, J. Grebowicz, H. Baur, *Adv. Polym. Sci.*, 1988, **87**, 1.
16. Yu. K. Godovsky, V. S. Papkov, *Adv. Polym. Sci.*, 1989, **88**, 129.
17. T. Verbiest, S. Van Elshocht, A. Persoons, C. Nuckolls, K. E. S. Phillips, T. J. Katz, *Langmuir*, 2001, **17**, 4685.
18. K. E. S. Phillips, T. J. Katz, S. Jockusch, A. J. Lovinger, N. J. Turro, *J. Am. Chem. Soc.*, 2001, **123**, 11899.
19. C. Nuckolls, T. J. Katz, *J. Am. Chem. Soc.*, 1988, **120**, 9541.
20. M. A. Shcherbina, X.-B. Zeng, T. Tadjiev, G. Ungar, S. H. Eichhorn, K. E. S. Phillips, T. J. Katz, *Angew. Chem.*, *Int. Ed. Engl.*, 2009, **48**, 7837.
21. W. Cochran, F. H. C. Crick, V. Vand, *Acta Crystallogr.*, 1952, **5**, 581.

22. R. E. Franklin, A. Klug, *Acta Crystallogr.*, 1955, **8**, 777.
23. V. Percec, C. M. Mitchell, W.-D. Cho, S. Uchida, M. Glodde, G. Ungar, X. Zeng, Y. Liu, V. S. K. Balagurusamy, P. A. Heiney, *J. Am. Chem. Soc.*, 2004, **126**, 6078.
24. V. Percec, M. N. Holerca, S. Uchida, W.-D. Cho, G. Ungar, Y. Lee, D. J. P. Yeardley, *Chem.—A Eur. J.*, 2002, **8**, 1106.
25. L. Vyklicky, S. E. Eichhorn, T. J. Katz, *Chem. Mater.,* 2003, **15**, 3594.
26. X. Zhu, M. A. Shcherbina, A. V. Bakirov, B. Gorzolnik, S. N. Chvalun, U. Beginn, M. Moller, *Chem. Mater.,* 2006, **18**, 4667.
27. X. Feng, M. E. Tousley, M. G. Cowan, B. R. Wiesenauer, S. Nejati, Y. Choo, R. D. Noble, M. Elimelech, D. L. Gin, C. O. Osuji, *ACS Nano*, 2014, **8**, 11977.
28. M. A. Shcherbina, A. V. Bakirov, L. Yan, U. Beginn, X. Zhu, M. Möller, S. N. Chvalun, *Mendeleev Commun.*, 2015, **25**, 142.
29. M. A. Shcherbina, A. V. Bakirov, A. N. Yakunin, U. Beginn, L. Yan, M. Möller, S. N. Chvalun, *Soft Matter*, 2014, **10**, 1746.
30. A. V. Bakirova, A. N. Yakunin, M. A. Shcherbina, S. N. Chvalun, X. Zhu, U. Beginn, M. Möller, *Rossiiskie nanotekhnologii* [*Russian Nanotechnologies*], 2010, **5**, 67 (in Russian).
31. U. Beginn, L. Yan, S. N. Chvalun, M. A. Shcherbina, A. Bakirov, M. Möller, *Liq. Cryst.*, 2008, **35**, 1073.
32. G. Natta, P. Pino, P. Corradini, *J. Am. Chem. Soc.*, 1955, **77**, 1708.
33. V. I. Selikhova, Ya. I. Odarchenko, N. P. Bessonova, E. A. Sinevich, M. A. Shcherbina, S. N. Chvalun, B. Rieger, *Polym. Sci., Ser. A*, 2015, **57**.
34. S. N. Chvalun, M. A. Shcherbina, I. V. Bykova, J. Blackwell, V. Percec, *Polym. Sci., Ser. A*, 2002, **44**.
35. Y.-K. Kwon, C. Danko, S. N. Chvalun, J. Blackwell, V. Percec, J. A. Heck, *Macromol. Symp.*, 1994, **87**, 103.
36. Y.-K. Kwon, S. N. Chvalun, A.-I. Schneider, J. Blackwell, V. Percec, J. A. Heck, *Macromolecules*, 1993, **27**, 6129.
37. Y.-K. Kwon, S. N. Chvalun, J. Blackwell, V. Percec, J. A. Heck, *Macromolecules*, 1995, **28**, 1552.
38. S. N. Chvalun, Y.-K. Kwon, J. Blackwell, V. Percec, *Polym. Sci., Ser. A*, 1996, **38**.
39. S. N. Chvalun, J. Blackwell, Y.-K. Kwon, V. Percec, *Macromol. Symp.*, 1997, **118**, 663.
40. S. N. Chvalun, J. Blackwell, J. D. Cho, Y. K. Kwon, V. Percec, J. A. Heck, *Polymer*, 1998, **39**, 4515.
41. S. N. Chvalun, J. Blackwell, J. D. Cho, I. V. Bykova, V. Percec, *Acta Polym.*, 1999, **50**, 50.
42. G. Ungar, Y. S. Liu, X. B. Zeng, V. Percec, W. D. Cho, *Science*, 2003, **299**, 1208.
43. D. C. Bassett, *Developments in Crystalline Polymers*, 1988, **2**, 346.
44. G. Ungar, *Macromolecules*, 1986, **19**, 1317.
45. S. N. Chvalun, M. A. Shcherbina, A. N. Yakunin, J. Blackwell, V. Percec, *Polym. Sci., Ser. A*, 2007, **49**.
46. C. H. M. Weber, F. Liu, X. B. Zeng, G. Ungar, N. Mullin, J. K. Hobbs, M. Jahr, M. Lehmann, *Soft Matter*, 2010, **6**, 5390.
47. G. Ungar, X. Zeng, *Soft Matter*, 2005, **1**, 95.
48. R. Williams, *Dover Pubns*, 1979, 265.
49. J. Charvolin, J. F. Sadoc, *J. Phys. I Fr.*, 1988, **49**, 521.
50. V. Luzzati, R. Vargas, A. Gulik, P. Mariani, J. M. Seddon, E. Rivas, *Biochemistry*, 1992, **31**, 279.
51. D. Weaire, R. Phelan, *Philos. Mag. Lett.*, 1994,**69**, 107.
52. P. E. Laibinis, G. M. Whitesides, D. L. Allara, Y. T. Tao, A. N. Parikh, R. G. Nuzzo, *J. Am. Chem. Soc.*, 1991, **113**, 7152.
53. M. Volmer, M. Stratmann, H. Viefhaus, *Surf. Interface Anal.*, 1990, **16**, 278.
54. K. Shimazu, Y. Sato, I. Yagi, K. Uosaki, *Bull. Chem. Soc. Jpn.*, 1994, **67**, 863.
55. J. C. Love, D. B. Wolfe, R. Haasch, M. L. Chabinyc, K. E. Paul, G. M. Whitesides, R. G Nuzzo, *J. Am. Chem. Soc.*, 2003,**125**, 2597.
56. D. L. Allara, R. G Nuzzo, *Langmuir*, 1985, **1**, 45.
57. D. L. Allara, R. G Nuzzo, *Langmuir*, 1985, **1**, 52.
58. C. W. Sheen, J. X. Shi, J. Martensson, A. N. Parikh, D. L. Allara, *J. Am. Chem. Soc.*, 1992, **114**, 1514.
59. N. L. Abbott, J. P. Folkers, G. M. Whitesides, *Science*, 1992, **257**, 1380.
60. M. Bollani, R. Piagge, D. Narducci, *Mater. Sci. Eng. C-Biomimetic Supramol. Syst.*, 2001, **15**, 253.
61. W. R. Ashurst, C. Yau, C. Carraro, R. Maboudian, M. T. Dugger, *J. Microelectromech. Syst.*, 2001, **10**, 41.
62. Q. L. Li, G. Mathur, M. Homsi, S. Surthi, V. Misra, V. Malinovskii, K. H. Schweikart, L. H. Yu, J. S. Lindsey, Z. M. Liu, R. B. Dabke, A. Yasseri, D. F. Bocian, W. G. Kuhr, *Appl. Phys. Lett.*, 2002, **81**, 1494.
63. S. Hong, R. Reifenberger, W. Tian, S. Datta, J. I. Henderson, C. P. Kubiak, *Superlattices Microstruct.*, 2000, **28**, 289.
64. C. B. Gorman, R. L. Carroll, R. R. Fuierer, *Langmuir*, 2001, **17**, 6923.
65. J. L. Wilbur, A. Kumar, E. Kim, G. M. Whitesides, *Adv. Mater.*, 1994, **6**, 600.
66. K. K. Berggren, A. Bard, J. L. Wilbur, J. D. Gillaspy, A. G. Helg, J. J. McClelland, S. L. Rolston, W. D. Phillips, M. Prentiss, G. M. Whitesides, *Science*, 1995, **269**, 1255.
67. M. J. Lercel, H. G. Craighead, A. N. Parikh, K. Seshadri, D. L. Allara, *Appl. Phys. Lett.*, 1996, **68**, 1504.
68. S. Q. Sun, G. J. Leggett, *Nano Lett.*, 2002, **2**, 1223.
69. J. A. Rogers, Z. Bao, M. Meier, A. Dodabalapur, O. J. A. Schueller, G. M. Whitesides, *Synth. Met.*, 2001, **115**, 5.
70. G. M. Whitesides, E. Ostuni, S. Takayama, X. Y. Jiang, D. E. Ingber, *Rev. Biomed. Eng.*, 2001, **3**, 335.
71. R. J. Jackman, J. L. Wilbur, G. M. Whitesides, *Science*, 1995, **269**, 664.
72. P. A. Smith, C. D. Nordquist, T. N. Jackson, T. S. Mayer, B. R. Martin, J. Mbindyo, T. E. Mallouk, *Appl. Phys. Lett.*, 2000, **77**, 1399.
73. T. Thurn-Albrecht, J. DeRouchey, T. P. Russell, H. M. Jaeger, *Macromolecules*, 2000, **33**, 3250.
74. H. Miguez, S. M. Yang, G. A. Ozin, *Langmuir*, 2003, **19**, 3479.
75. X. L. Xu, S. A. Majetich, S. A. Asher, *J. Am. Chem. Soc.*, 2002, **124**, 13864.
76. A. Corma, *Chem. Rev.*, 1997, **97**, 2373.
77. J. Y. Ying, C. P. Mehnert, M. S. Wong, *Angew. Chem., Int. Ed. Engl*, 1999, **38**, 56.
78. M. E. Davis, *Nature*, 2002, **417**, 813.
79. Y. Wan, D. Y. Zhao, *Chem. Rev.*, 2007, **107**, 2821.
80. J. S. Beck, J. C. Vartuli, W. J. Roth, M. E. Leonowicz, C. T. Kresge, K. D. Schmitt, C. T. W. Chu, D. H. Olson, E. W. Sheppard, S. B. McCullen, J. B. Higgins, J. L. Schlenker, *J. Am. Chem. Soc.*, 1992,**114**, 10834.
81. P. T. Tanev, T. J. Pinnavaia, *Science*, 1995, **267**, 865.
82. Q. S. Huo, D. I. Margolese, U. Ciesla, P. Y. Feng, T. E. Gier, P. Sieger, R. Leon, P. M. Petroff, F. Schuth, G. D. Stucky, *Nature*, 1994, **368**, 317.

83. D. Y. Zhao, J. L. Feng, Q. S. Huo, N. Melosh, G. H. Fredrickson, B. F. Chmelka, G. D. Stucky, *Science*, 1998, **279**, 548.
84. S. Che, A. E. Garcia-Bennett, T. Yokoi, K. Sakamoto, H. Kunieda, O. Terasaki, T. Tatsumi, *Nat. Mater.*, 2003, **2**, 801.
85. Y. Wan, H. F. Yang, D. Y. Zhao, *Acc. Chem. Res.*, 2006, **39**, 423.
86. J. Lee, J. Kim, T. Hyeon, *Adv. Mater.*, 2006,**18**, 2073.
87. Y. Wan, Y. Shi, D. Zhao, *Chem. Mater.*, **20**, 932.
88. M.-H. Yen, J. Chaiprapa, X. B. Zeng, Y. S. Liu, L. Cseh, G. H. Mehl, G. Ungar, *J. Am. Chem. Soc.*, 2016, **138**, 5757.

Received February 14, 2018;
in revised form June 26, 2018;
accepted July 30, 2018